

# Impact of Intense Pico second Pulsed Electric Fields on Melanoma Cells by the Irradiation of UWB Antenna

Petrishia.A<sup>1</sup>, Sasikala.M<sup>2</sup>

<sup>1</sup>Department of ECE, Anna University, Chennai. Tamilnadu, India.

<sup>2</sup>Department of ECE, Anna University, Chennai. Tamilnadu, India

**ABSTRACT**—The Intense pulsed Electromagnetic field can treat melanoma cells. This way of treating cancerous cells ensures very less radiation on the normal part of our body. In this work the tapered arm Impulse Radiating Antenna (IRA) is designed with high gain. The IRA with tapered feeding arms located at the position of  $\phi=60^\circ$  gives an average gain improvement of 14% with traditional IRA. Its Electric field distribution has a 3dB beam width of 2 cm and 1cm along lateral and axial direction respectively. The electric intensity radiated by the antenna is 25kV/cm for the input of 130kV. The abnormal skin model is defined and the effect of application of the picosecond pulse is studied at elevated temperature. The temperature at the tumor location is 1.8% higher than the nearby tissue for an input of 1 V.

**INDEX TERMS**—Melanoma cells, Prolate Spheroidal Impulse Radiating Antenna (PSIRA), Picosecond Electric Pulse (PsEP).

## I. INTRODUCTION

The research of dielectric has moved in to pulse range of subnanoseconds. The understanding of the interaction of subnanosecond pulses and cells or tissues, however, is relatively poor compared with that of microsecond and nanosecond pulses. The cells expose to picosecond pulses undergo a cell death. The pulse generators of 100ps-200ps long, several hundreds of kilovolts in amplitude, have become commercially available (FID Technology). The Impulse Radiating Antennas are used to irradiate such pulses. The high gain antennas are used for effective focus of the picosecond pulses in the near field where the target (skin phantom) is present.

However, there are two reasons to enter the picoseconds-pulsed electric field range. The first one is

that for extremely short pulses, the permittivity of the various cellular components, rather than their resistivity,

determines the electric field distribution in the cell. The electric field then acts directly on membrane proteins, rather than causing charging of the membrane, and, if sufficiently strong, can cause direct and instant conformational changes. Sub nanosecond pulses (100 ps) were found to alter the cell membrane conductance and unrectifying channels are formed when cells are exposed to electric field strength on the order of 20 kV/cm for 2000 pulses. The disruption of the membrane integrity may lead to the change of physiological conditions of the cell and cause cell death. Second, besides providing the opportunity to explore a new field of electric field-cell interactions, subnanosecond pulses will ultimately allow medical applications for delivery of pulsed electric fields without invasive electrodes, using antennas instead. [1][2].

A Prolate Spheroidal Impulse Radiating Antenna (PSIRA) is used to focus the picosecond pulsed electric field in the near field [3]. In order to enhance the gain of the PSIRA the feed arms are tapered. The PSIRA is fed at the first focal point and the target is placed at the second focal point. The waves coming out of the reflector are spherical and converging to the second geometric focus where the cancerous tissue is present.

Thomas Camp et al. shows that the exposure of Hepa 1-6 cells to 2000 pulses of 200ps duration and electric field amplitudes exceeding 80kV/cm induced cell death is almost 30% of the cells when the temperature is increased to 47 °C for the time of pulsing using electrodes as a pulse delivery system [4]. In this work PSIRA with tapered feed arm is used to launch 100ps pulses. At the tumor location the temperature is raised when the pulses are launched from the first focal point of the PSIRA. Due to the elective focus the antenna the temperature at the tumor location is higher than the nearby tissue.

This paper is organized as follows. In section II we present the traditional Prolate Spheroidal Antenna design. In section III shows an enhanced design of feed arms. Section IV is described about Skin model description and effects of biological material under the influence of electric field.

**II TRADITIONAL PSIRA  
A NON INVASIVE CANCER TREATMENT TOOL**

The Impulse radiating antenna is a focused aperture ultra-wideband antenna suited for radiating very fast high-voltage 100-kV pulses in a narrow beam. IRAs thus provide an attractive means to deliver electrical pulses to induce apoptosis in tissue cells without using needles. [5]

*A. Antenna configuration*

The antenna consists of three elements, a Prolate spheroidal reflector, a tapered conical feed structure and a balun. The aperture of the reflector minor axis is 25cm. The semi major axis is 29.8cm. [6] An in homogenous spherical TEM wave launched on guiding conical conductors from one focus is focused into the second focal point, where the target is placed. The focal distance so is 16.3cm. [6]. The feed arms are placed 60° with respect to the y axis. A balun made of two 100Ω cables, allows a 1:4 ratio impedance transformation from the pulse input to the conical transmission line. Refer Fig.1

*B. Design Equations*

The antenna consists of a parabolic reflector with a focal length of *f* and diameter of *D*. A pair of cross conical coplanar TEM transmission lines is used to realize the feeding structure. The feeding arms originate at the focal point and terminate at the rim of the parabolic reflector through the termination loads. The conically symmetric TEM feeding structure parameters [ $\beta_0, \beta_1, \beta_2$ ] are related to the equivalent longitudinally symmetric structure parameters (*a, b1, b2, D, F*) through a combined method of stereographic projection and conformal mapping. Refer Fig. 2.

The feed impedance of TEM feed [9]

$$f_g = K(m)/2K(1-m)$$

*K* (*m*) is the elliptical integral of the first kind.

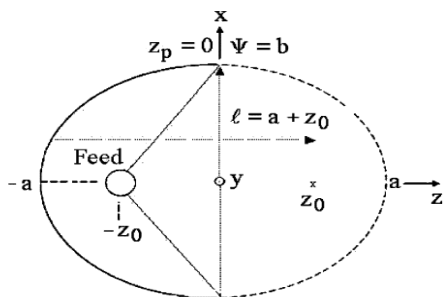


Fig. 1. Side view of a Prolate Spheroid reflector antenna

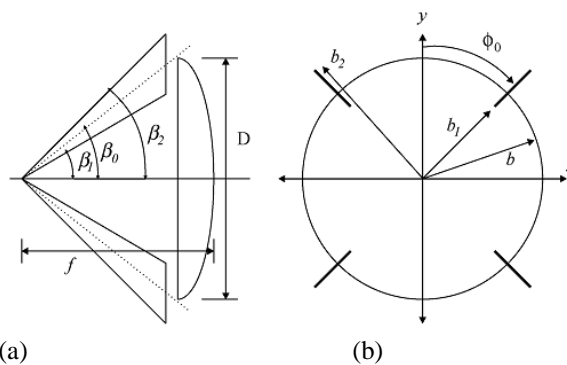


Fig.2. (a) Side view with focal length and diameter. (b) Aperture plane after stereographic projection.

$$\beta_0 = \arctan[(1/2f/D - D/8f)]$$

$$\beta_1 = 2 \arctan(m^{1/4} \tan(\beta_0/2))$$

$$\beta_2 = 2 \arctan(m^{1/4} \tan(\beta_1/2))$$

$$b_1/a = \tan(\beta_1/2) / \tan(\beta_0/2)$$

$$b_2/a = \tan(\beta_2/2) / \tan(\beta_0/2)$$

$$a = \sqrt{b_1 b_2}$$

The Prolate spheroidal reflector type IRA can radiate a picosecond pulse that is highly directive. The antenna is also efficient because of radiates large portion of the input energy. The TEM feed arms have a conical geometry within a sphere of radius *L* centered at the focal point spherical TEM wave launched at the drive point propagates outward without disturbance.

**III ENHANCED DESIGN OF FEED ARM**

*A. Feeding Structure at the focal point*

Performance of the Impulse Radiating antenna at high frequency is very sensitive to the feeding structure design at the focal point. Due to the conical property of the coplanar TEM feeding structure, the width of each arm goes to zero at the focal point. It is very difficult when we connect coaxial cable with non-zero feeding arm at the focal point. So the Prolate spheroidal reflector has two pair of tapered coplanar plate feed arms which are placed 60° to each other.

*B. Tapered Feed arm with phi\_0 = 60°*

We constructed impulse radiating antenna using a 50 cm diameter based on four tapered feed arm with phi\_0 = 60°. In order to reduce the energy stored around the junction of the reflector and feed arms and to improve the gain of IRA to focus the target tissue without affecting nearby tissue, the end part of the feeding arms are tapered. [7]. Fig.3 shows the traditional and tapered feed arm.

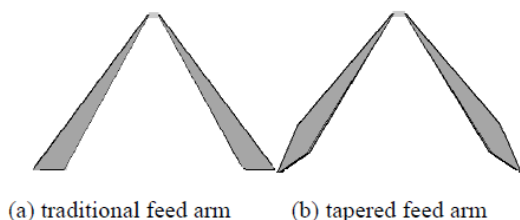


Fig.3. Traditional and tapered feed arm.

IV.SKIN MODEL DESCRIPTION

A. Two layer skin model

The skin model chosen in this case has been set up with a specific length and width. This is a two layer model which consists of the epidermis and dermis with the thickness of 0.15mm and 3.85mm respectively. Also air layer is included above the skin layers. The length and width of the phantom have been specified by 5cm x 5 cm. The tumor model is chosen as a square with the area of 2 cm<sup>2</sup>. The phantom is kept at the distance of 46.1cm (second focal point) from the antenna vertex.

Details of the dielectric properties of the normal skin phantom model and tumor which is used for our simulation is given in Table. I.[8]-[11].

TABLE.I  
DIELECTRIC PROPERTIES OF PHANTOM MODEL

S. No	Properties	Air	Epidermis	Dermis	Tumor
1	Dielectric constant	1	38.007	38.007	78
2	Conductivity (S/m)	1	0.2	0.2	0.89
3	Material Density (Kg/m <sup>3</sup> )	1.204	1100	1100	1040
5	Thermal Conductivity (W/K/m)	0.026	0.5	0.5	
6	Heat capacity (KJ/K/kg)	1.005	3.35	3.35	3.9
7	Basal metabolic rate (W/m <sup>2</sup> )		-	200	

V.RESULTS AND DISCUSSION

A. Performance of PSIRA with Tapered Arm

Fig.4 shows that a Prolate Spheroidal reflector and two feed arm over a ground plane. A 1V of 100ps pulses is launched from the first focal point. The modeling results show that the pulse radiation is focused at the second focal point where the target (skin phantom) is located. According to the electrical properties, the two layer skin model is defined with the thickness of 4 mm below the layer of air. The gain of the PSIRA with tapered arm is increased as 28.1 dB as compared to traditional arm. It is shown in Fig.5 and 6. The 3 dB

angular width is 4.7°. The VSWR value is shown in Fig.7 which is less than 2 for the band of 0 to 15 GHz.

The electric field intensity is plotted as a function of distance from the focal point. The spot diameter can be measured from the lateral and axial field distribution. The distribution of field intensity has a 3-dB beamwidth of 2 cm in lateral direction and 1 cm in axial direction (z=16.3 cm) which is shown in Fig 8 and Fig .9 respectively. We also noted that the maximum of the impulse electric field on the axis is shifted slightly from the geometric focus (z=16.3 cm) towards the reflector. This is because the impulse decreases inversely with distance while it is focused in space. A pulse with faster rise time should allow the shift of the focal spot towards the geometric focus.

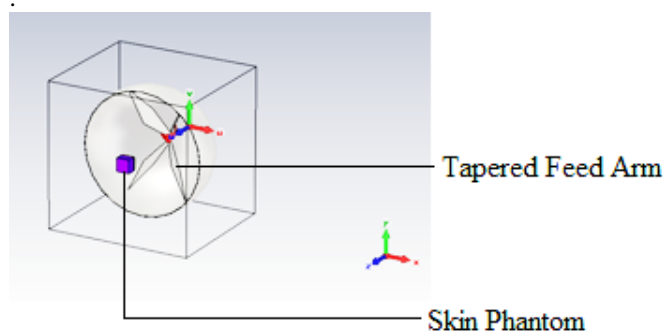


Fig.4. Prolate Spheroidal IRA with Skin Phantom model

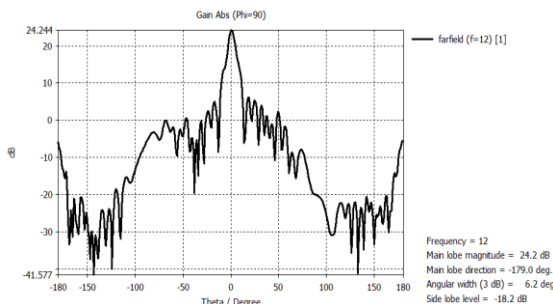


Fig.5. 2D plot of radiation pattern shows the gain of 24.2dB

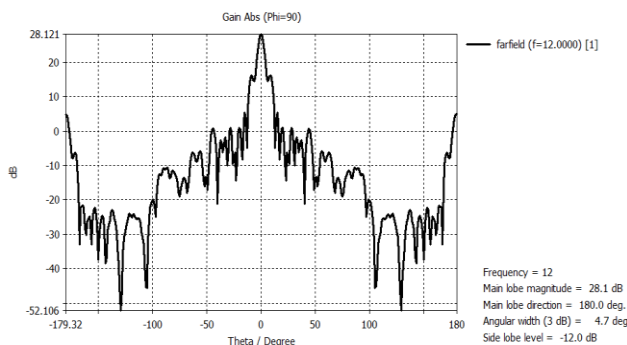


Fig.6. 2D plot of radiation pattern shows the gain of 28.1 dB.

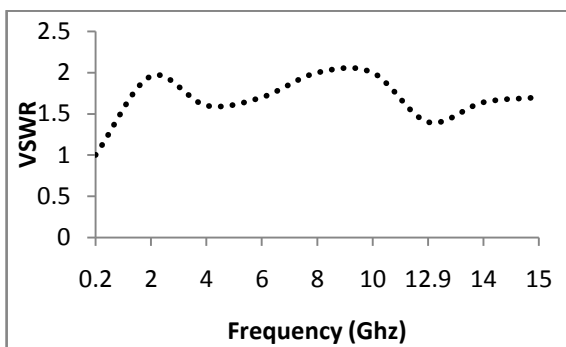


Fig.7.VSWR Value of IRA

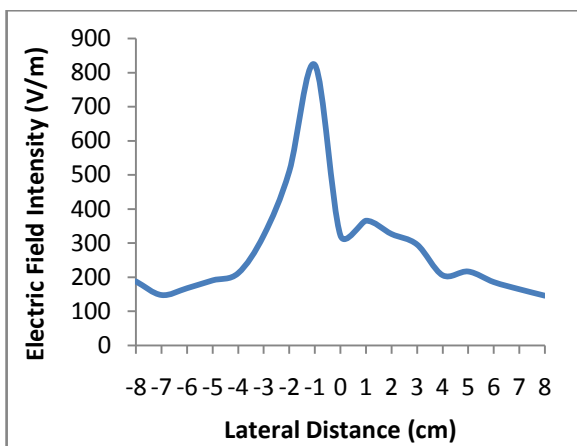


Fig.8 Peak Electric field as a function distance along the y-axis focus (lateral direction)

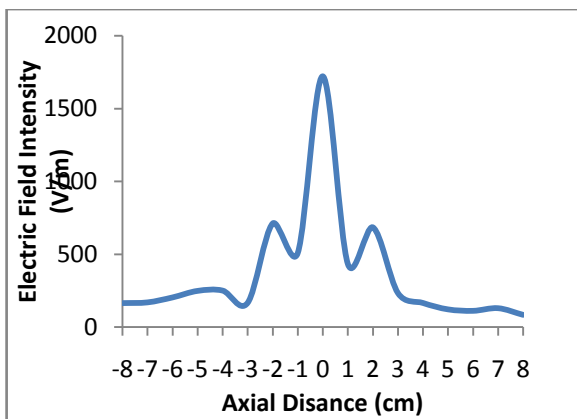


Fig.9 Peak Electric field as a function distance along the z- axis focus (axial direction)

*B. Effects of Picosecond pulse on skin phantom model*

In this section we can study the skin phantom model with and without tumor. The high background electric field is typically used in simulations. If the microwave power is increased, but at a decreased exposure time such that the total deposited energy is less than that used to generate hyperthermia, we can expect both electrical effects (due to the high power level) and also effects

which are caused by the rapid rise of heating, even if the total temperature is below the level of hyperthermia. Studying the cell death with increasing temperature rate of rise we have observed a strong nonlinear effect. By increasing this rate, the death rate of liver cancer cells in suspension was found to increase with a power law. [12]. The temperature distribution is studied by the application of electric field intensity. The temperature at the tumor location is 0.6% higher than the nearby tissue, because of the effective focus of PSIRA with small spot diameter. With 2000 pulses at 20kV/cm a temperature of the biological model of 47° C is raised. Fig.10 and Fig.11 show that the temperature raises for skin phantom with and without tumor. Fig.12 shows that the electric field at the second focal point by the application 130kV as the input. The radiated electric field intensity at the second focal point is 24kV/cm.

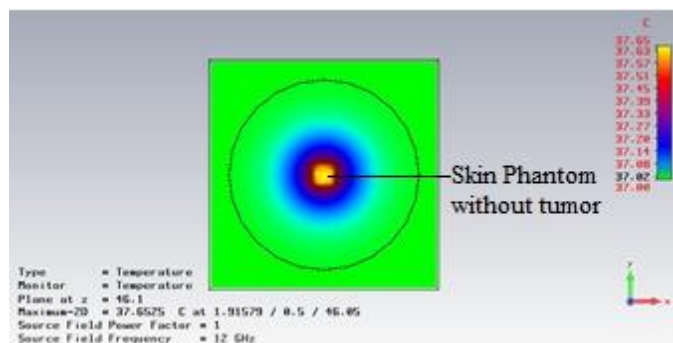


Fig.10 Temperature distribution of skin phantom without tumor

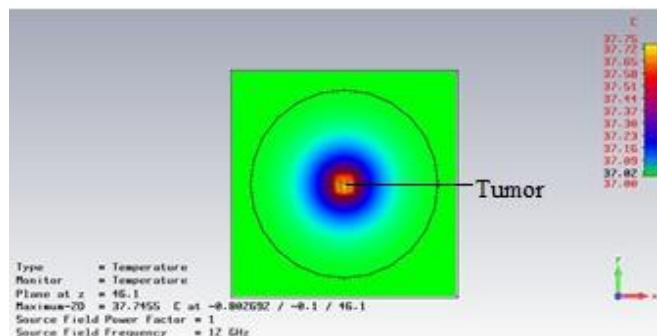


Fig.11 Temperature distribution of skin phantom with tumor

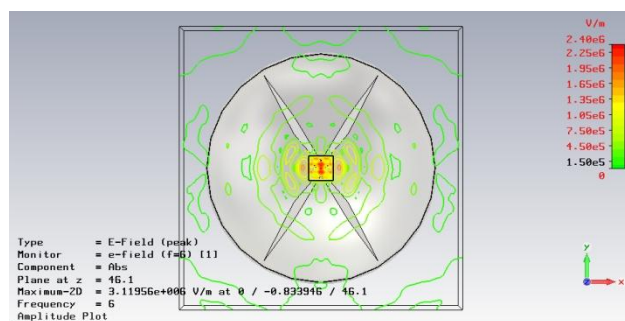


Fig.12.Radial distribution of Electric Field at second focal point with the input of 130kV.

The presence of tumor at the focus location introduces a local increase in the absorbed power density due to higher conductivity of the tumor relative to the surrounding tissue. This selective absorption of the tumor enhances the inherent focusing capacity of the radiator.

Pulsed electric fields have been used to induce a biological response in cells, and a sufficient energy, can cause cell death. Studies have previously been completed in which the aim was to determine the energy density required to induce cell death with 800s pulses. In his work, it is shown that the energy density required for cell death can be reduced considerably if the temperature of the sample is increased to values above physiological temperature.

## VI CONCLUSION

The Prolate spheroid reflector antenna is studied with improving structure. According to the simulation result the gain of the antenna is increased in order to improve the performance of the antenna compared to the traditional IRA. The impulse radiating antenna with tapered feed arm reduces the beam width which is used to exactly locate the target area. The IRA with tapered arm produces 28.1 dB and temperature profile of abnormal skin for skin cancer treatment by the application of impulse electric field is discussed. The temperature at the focal point is higher where the tumor is located because of the effective focus of the impulse radiating antenna. Generally, in studies of the bioelectric effects of nanosecond and subnanosecond pulses, thermal effects are not considered. This is certainly true for single pulse experiments or multiple pulse experiments with a small number of pulses at a low repetition rate. However, applications of such effects of medical treatments based on tissue ablation, such as skin cancer treatments require multiple pulses applied at a high repetition rate.

The effect of temperature increase for such high repetition rate, pulse sequence should not be neglected. Rather than having a negative effect on the medical treatment, short-term temperature increases of several degrees Celsius above the physiological temperature, generated either by the pulses themselves or produced through external, local heating, may allow a considerable reduction in the pulse number and amplitude for these treatments. In our studies, we have found that temporary heating of the cells to temperatures less than 10° C above the physiological temperature does not cause cell death (for exposures of ten minutes and less). However, this temporary increase in temperature allows us to reduce the specific energy of the electrical pulses required for inducing cell death by orders of magnitude compared to using the pulses at physiological temperature and below.

## REFERENCES

- [1] R. Nuccitelli, U. Pliquett, X. Chen, W. Ford, J. Swanson, S. J. Beebe, J. F. Kolb, and K. H. Schoenbach "Nanosecond pulsed electric fields cause melanomas to self-destruct," *Biochem. Biophys. Res. Commun.*, vol. 343, no. 2, pp. 351–360, May 2006.
- [2] K. H. Schoenbach, B. Hargrave, R. P. Joshi, J. F. Kolb, C. Osgood, R. Nuccitelli, A. Pakhomov, R. J. Swanson, M. Stacey, J. A. White, S. Xiao, J. Zhang, S. J. Beebe, P. F. Blackmore, and E. S. Buescher, "Bioelectric

- effects of intense nanosecond pulses," *IEEE Trans. Dielectric Elect. Insul.*, vol. 14, no. 5, pp. 1088–1119, Oct. 2007.
- [3] S. Xiao, S. Altunc, P. Kumar, C. E. Baum, and K. H. Schoenbach, "A reflector antenna for focusing in the near field," *IEEE Antennas Wireless Propag. Lett.*, Vol. 9, pp. 12–15, 2010
- [4] J. Thomas Camp, Yu Jing, Jie Zhuang, Juergen F. Kolb, Stephen J. Beebe, Jiahui Song, Ravindra P. Joshi, Shu Xiao, and Karl H. Schoenbach "Cell Death Induced by Subnanosecond Pulsed Electric Fields at Elevated Temperatures" in *IEEE Transactions on Plasma Science*, Vol. 40, no. 10, October 2012.
- [5] K. H. Schoenbach, S. Xiao, J. T. Camp, M. Migliaccio, S. J. Beebe and C. E. Baum "Wideband High-Amplitude, Pulsed Antenna for Medical Therapies and Medical Imaging," *International Conference on Electromagnetics In Advanced Applications* in Torino, 14-18 September, 2009.
- [6] Prashanth Kumar, Carl E. Baum, Serhat Altunc, Jerald Buchenauer, Shu Xiao, Christos G. Christodoulou, E. Schamiloglu, and Karl H. Schoenbach, "Hyperband Antenna To Launch and Focus Fast High-Voltage Pulses Onto Biological Targets" *IEEE Transaction on Microwave Theory and Techniques*, VOL. 59, NO. 4, APRIL 2011
- [7] Majid Manteghi and Yahya Rahmat Samii "Improved Feeding Structures to enhance the performance of the Reflector Impulse Radiating Antenna (IRA)" *IEEE Transaction on Antenna and Propagation* Vol. 54. No. 3, March 2006.
- [8] Nacer Chahat, Maxim Zhadobov, Ronan Sauleau, and Stanislav I. Alekseev, "New Method for Determining Dielectric Properties of Skin and Phantoms at Millimeter Waves Based on Heating Kinetics" *IEEE Transactions on Microwave Theory and Techniques*, vol. 60, no. 3, March 2012
- [9] ITALIAN NATIONAL RESEARCH COUNCIL-Institute for Applied Physics-Web site
- [10] <http://niremf.ifac.cnr.it/tissprop/http://www.aqua-calc.com/page/density-table/substance/human-blank-body>.
- [11] Frank Gustrau and Achim Bahr "W-Band Investigation of Material Parameters, SAR Distribution, and Thermal Response in Human Tissue" *IEEE Transaction on Microwave Theory And Techniques*, VOL. 50, NO. 10, October 2002.
- [12] J. T. Camp, S. Xiao, H. Baldwin, and K. H. Schoenbach, "Effect of the Rate of Temperature Increase on Liver Cancer Cells in Vitro," Power Modulator and High Voltage Conference 2010, Atlanta, GA.